Mem. S.A.It. Vol. 90, 413

Memorie della

White dwarf binaries in the Milky Way

A. Lamberts

Observatoire de la Côte d'Azur, 96 Boulevard de l'Observatoire, 06300 Nice, France
e-mail: astrid.lamberts@oca.eu

Abstract. White dwarf binaries with orbital periods below one hour will be the most numerous sources for the space-based gravitational wave detector *LISA*. Based on thousands of individually resolved systems, we will be able to constrain binary evolution and provide a new map of the Milky Way and its close surroundings. In this presentation we show the main properties of populations of different types of detached white dwarf binaries detected by *LISA* over time. We combine a high-resolution cosmological simulation of a Milky Way-mass galaxy with a binary population synthesis model for low and intermediate mass stars. Thanks to the simulation, we show how different galactic components contribute differently to the gravitational wave signal, mostly due to their typical age and distance distributions. We find that the dominant *LISA* sources will be He-He double white dwarfs (DWDs) and He-CO DWDs with important contributions from the thick disk and bulge. The resulting sky map of the sources is different from previous models, with important consequences for the searches for electromagnetic counterparts, possibly with *Gaia* or LSST.

Key words. Stars: white dwarfs, binaries – Galaxy: stellar content– Gravitational waves

1. Introduction

Gravitational waves (GW) are the most promising way towards systematic detection of compact binaries. Within the next 20 years the *Laser Interferometer Space Antenna (LISA)* will open up a new window in the GW spectrum, between 10^{-5} and 10^{-2} Hz (Amaro-Seoane et al. 2017). By numbers, the dominant sources for *LISA* will be double white dwarfs (DWD) in our Milky Way (MW), about a hundred thousand years before they merge. As white dwarfs (WD) are the remnants of stars below $\lesssim 8M_{\odot}$, more than 95% of the stars are likely to end their lives as WDs.

In a seminal paper, Nelemans et al. (2001b) determined several tens of millions of detached DWDs would be present in the *LISA* band and roughly ten thousand of them, with GW frequency $f_{GW} \gtrsim$ 0.4 mHz, would be individually resolvable. With (at least) thousands of detectable systems, *LISA* will allow new statistical studies of close DWDs. Such studies will strongly advance our understanding of stellar and binary evolution. GW observations are very complementary to electromagnetic (EM) observations, which are challenging as WDs are faint and rapidly cool down to become even fainter. Even with dedicated surveys, our view of DWDs in the MW is going to be hindered by dust extinction and faintness of the sources before the start of *LISA* operations. Short period binaries observable by *LISA* (orbital period below half an hour) are found with phase-resolved spectroscopy of previously discovered white dwarfs (Napiwotzki et al. 2001; Brown et al. 2010, 2016) or light curves from

high cadence surveys (Levitan et al. 2013). These electromagnetically identified binaries are called "verification binaries" and are guaranteed multi-messenger sources (see Kupfer et al. 2018, for an updated list using *Gaia* distances). Large scale systematic searches for these high frequency systems are just starting, withe e.g. the high cadence survey ZTF (Zwicky Transient Factory; Bellm et al. 2019; Graham et al. 2019) and possibly LSST (Large Synoptic Survey Telescope).

DWDs will be a new way to look at our MW, showing a population of older, low mass stars. As the strain amplitude of GW decreases only as $1/r$ (in comparison to $1/r^2$ decrease for electromagnetic emission), *LISA* will be able to more easily sample more remote regions of our Galaxy, its satellite and maybe Andromeda (Cooray & Seto 2005; Korol et al. 2018). The *LISA* detections could lead to a new measurement of the Galactic potential (Korol et al. 2019) and the global amplitude of the signal due to DWDs will quantify the star formation history of the MW (Yu & Jeffery 2013).

Since the first predictions based on a Galaxy model combined with a binary population model (Nelemans et al. 2001b,a), models have included detailed studies of different DWD formation channels (Nissanke et al. 2012), the different types of DWDs and their spatial distribution in the MW (Ruiter et al. 2010). Important uncertainties remain regarding binary evolution (Postnov & Yungelson 2014), although the volume of observational completeness in our neighbourhood is slowly increasing and is a promising way to put constraints (Toonen et al. 2017). More recent studies demonstrate the potential of multi-messenger detections and the link with *Gaia* and LSST (Korol et al. 2017; Breivik et al. 2018). Korol et al. (2019) predicts that *Gaia* will detect about 25 verification binaries within 2 kpc, and LSST about 50 more, within 10 kpc; and that most of them will be away from the Galactic plane and bulge.

All these studies are based on parameterised models for the MW's star formation and structure. They use parameterised models for star formation and axisymmetric models for the different components of the galaxy, which often only model the thin disk and bulge. Ruiter et al. (2009) first highlighted that different galactic components have different contributions to the GW signal because of their different age, metallicity and typical distances. We combine a binary population synthesis model with a cosmological hydrodynamic simulation of a MW-like galaxy (Wetzel et al. 2016) to model the structure and star formation history. This allows us to naturally include all the components of the MW such as the thin and thick disk, the bulge and the accreted stellar halo, as well as a population of satellite galaxies. A similar approach for binary black holes (Lamberts et al. 2018) has shown that the latter are over-represented in the stellar halo of the galaxy, where the metallicity is low.

2. Method

We follow the same method as Lamberts et al. (2018), built on a set of simulations of MW-like galaxies and a binary population synthesis mode uniquely combined together to make GW predictions.

The FIRE Galaxy model We use of MW-like the "Latte" simulation; Wetzel et al. 2016 from the Feedback in Realistic Environment (FIRE; Hopkins et al. 2014) project[1]. These simulations are based on the improved "FIRE-2" version of the code from Hopkins et al. (2018, for details, see Section 2 therein) and ran with the code GIZMO (Hopkins 2015)[2]. These simulations have an initial gas particle mass of about 7070 $M_\odot$ and for the gas, both the hydrodynamic and gravitational resolutions are fully adaptive down to 1 pc. All the binary evolution models are included during post-processing, and the hydrodynamic simulation does not explicitly include binary effects. **m12i** shows metallicity gradients (Ma et al. 2017) and abundances of α-elements (Wetzel et al, in prep.) in the disk that are broadly consistent with observations of the MW. Its global star

[1] `http://fire.northwestern.edu`

[2] `http://www.tapir.caltech.edu/~phopkins/Site/GIZMO.html`

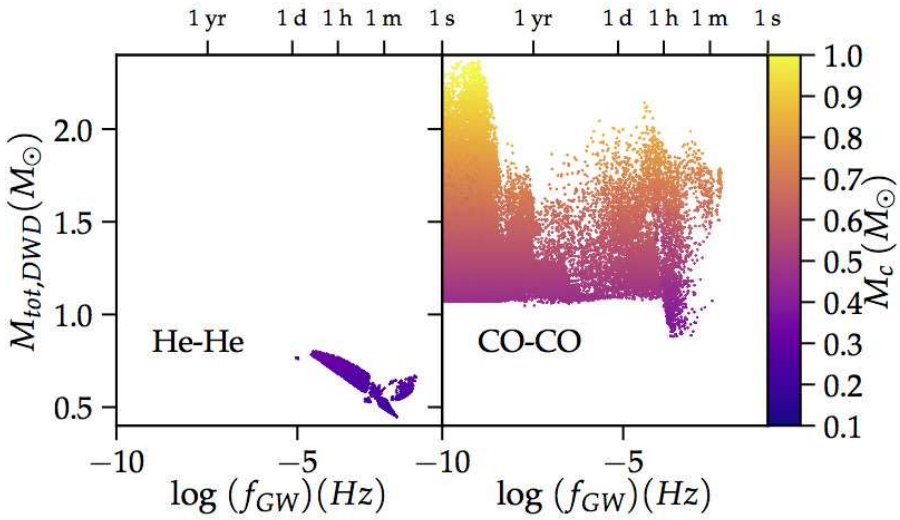

Fig. 1. Final periods and masses for a binary evolution model with 2.5 million binaries for $Z = Z_\odot$. We only show He-He and CO/CO DWDs for illustration. We show the gravitational wave frequency $f_{\rm GW}$ and orbital period $P_{\rm orb}$ at the formation of the binary and its total mass $M_{\rm tot,DWD}$. The colour shows the chirp mass M_c which is relevant for detectability with *LISA*.

formation history is consistent with the MW (see Ma et al. 2017 for illustrations) although its present day star formation rate of $6M_\odot$ yr^{-1} is somewhat higher than observed in the Milky Way. The satellite distribution around the main galaxy in **m12i** presents a similar mass and velocity distribution as observed around the Milky Way and M31, down to a stellar mass of $10^5 M_\odot$, though the simulation does not contain an equivalent of the Large Magellanic Cloud; the most massive satellite is comparable to the Small Magellanic Cloud.

From the simulation, we recover the position, formation time t_*, metallicity Z and position and mass at formation M_* of every star particle. We only use the particles within 300 kpc of the centre of the galaxy. This is slightly larger than the virial radius of the galaxy and allows us to largely sample the halo, satellites and streams while remaining unaffected by the boundaries of the high resolution region. This yields a list of roughly 14 million star particles.

Binary Population Synthesis model (BPS) To simulate a population of DWDs, we use a modified version of the publicly available `BINARY STAR EVOLUTION (BSE)` code based on the rapid binary evolution algorithm described in Hurley et al. (2002). For low mass binaries (see Postnov & Yungelson 2014, for a recent review), the main uncertainty stems from our limited understanding of the common envelope phase (Ivanova et al. 2013). We model 13 logarithmically spaced metallicity bins between 5×10^{-3} and $1.6Z_\odot$. We model a distribution with a thermal eccentricity and model a distribution of initial separations between 1 $R_\odot$ and $10^6 R_\odot$ following a flat distribution in log space. Primary masses m_{1*} are drawn from a Kroupa IMF (Kroupa 2001) between $0.95 < m_{1*} < 10M_\odot$ and secondary masses are set by $m_2 = qm_1$ where q is uniformly distributed between 0 and 1. We discard binaries with $m_{2*} < 0.5M_\odot$ as lower mass secondaries will not form DWDs within a Hubble time. With this condition, more than 90 percent of the systems are discarded, saving significant computing time.

There are many important uncertainties, especially for the impact of mass transfer. In this work, we have chosen standard values for the binary and stellar evolution. As our focus is the combination with an updated model for the

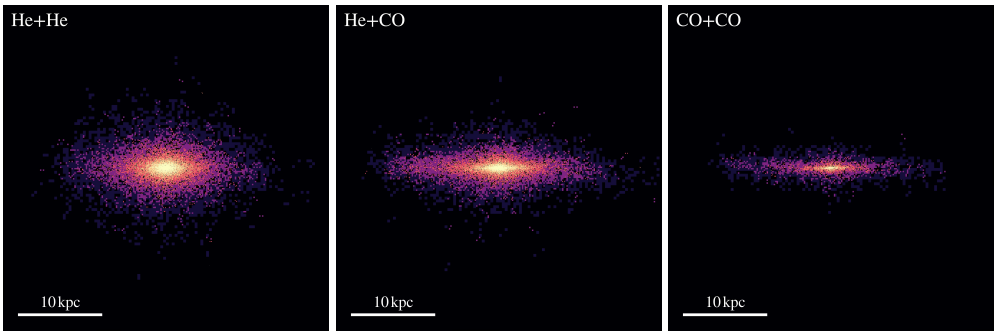

Fig. 2. Maps of the He-He DWDs (left), He-CO (middle) and CO-CO DWDs (right) viewed and edge-on. These maps only show the binaries with $f_{GW} > 10^{-3}$ Hz, which are the most likely to be individually resolved by *LISA*. Their distribution is very similar to the COCO binaries.

Milky Way rather than binary evolution, we restrict ourselves to this single set of parameters and leave a wider exploration for further work. For each metallicity, we eventually produce a list of DWDs with their formation time after the formation of the progenitor binary, their orbital properties and masses. With 2.5 million initial binaries in the appropriate mass range, we end up with about 700 000 DWDs in each metallicity bin. For a binary fraction of 0.5 we find a DWD formation rate of 0.012-0.016 DWDs per unit Solar mass of total star formation (including binaries and singles). There is limited variation with metallicity.

We identify He (helium) WDs, CO (carbon/oxygen) WDs and Ne (neon) WDs separately. These different populations stem from different progenitor masses and/or binary evolution channels. Different sub-types of WDs have different radii and cooling times, which is important for their electromagnetic properties. In this paper we will show that different sub-types also contribute differently to the GW signal.

Fig. 1 shows the masses and orbital periods at the formation of the He-He and CO-CO binaries as computed by `BSE` for an initial population at Solar metallicity. He-He WD come from two low-mass stars, which evolve very slowly, and have both their envelopes stripped by common envelope interactions. He-He DWDs stem from binaries with short initial periods and constitute a small fraction of the total population of DWDs, but they are important for *LISA*. The formation time of these binaries is rather constant between 2 and 13 Gyr. This results in low mass WDs ($M_{WD} < 0.45\ M_{\odot}$) in a very tight orbit. CO-CO WDs come from initially wider orbits, preventing the stripping of the envelope before the beginning of core He burning, and resulting in CO cores. Most of these systems have never interacted and will always have a large separation, which makes them less relevant for *LISA*. CO-CO binaries form in less than a Gyr and make up the bulk of the DWD population, with masses above $0.45 M_{\odot}$ (and often above $0.65 M_{\odot}$) and periods down to one hour. All binaries observable by LISA have recently become DWDs or they would have merged already.

Combining the galaxy and binary model for GW populations Each star particle within $\simeq$ 300 kpc) gets assigned n_{DWD} white dwarf binaries, depending its stellar mass at birth M_* and its metallicity (although the impact of metallicity is limited). All the DWDs are stored in a dataframe. We randomly draw with replacement n_{DWD} from our BPS model for each star particle and add them to the dataframe. The DWDs inherit the formation time and metallicity of the progenitor star as well as its current position and position at formation. The formation time of the DWD is the sum of the formation time of the progenitor and of the DWD. DWDs with formation times beyond the present day are removed (about 50% of the initial sample). We forward model the binaries until the present day via gravitational wave ra-

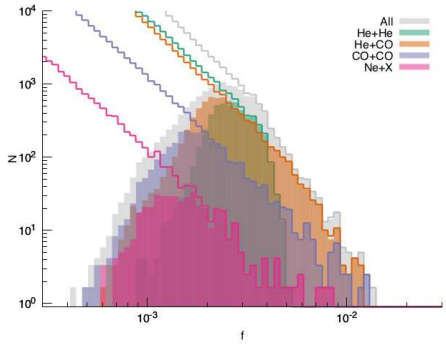

Fig. 3. Frequency distribution of the systems with S/N>7 in comparison with the total distribution after an eight-year observing time. Note that the catalogue of detected binaries with $f_{\rm GW} \gtrsim 3$ mHz ($f_{\rm GW} \gtrsim 2$ mHz for the more massive UCBs), is complete.

diation, gradually shortening the orbit. We remove binaries that have already merged (less than 10% of the sample).

To estimate the capability of *LISA* to detect and characterise white dwarf binaries in the galaxy models, we simulate the *LISA* data by co-adding the gravitational waveforms from all binaries with signals in the measurement band using the fast waveform generator in Cornish & Littenberg (2007). The dimensionless GW strain from a compact binary at a distance r is given by

$$h = 2(4\pi)^2 f_{\rm GW}^{2/3} \frac{G^{5/3}}{c^4} \frac{M_c^{5/3}}{r}. \quad (1)$$

The measurement of the GW strain and frequency alone are insufficient to determine the chirp mass of the binary, which is degenerate with the distance. The chirp mass (and therefore distance) can be determined for galactic binaries in the *LISA* band, having wide orbital separations and orbital velocities $\ll c$, to leading order in the frequency evolution

$$M_c = \frac{c^3}{G} \left(\frac{5}{96} \pi^{-8/3} f_{\rm GW}^{-11/3} \dot{f}_{\rm GW} \right)^{3/5} \quad (2)$$

assuming that other contributions to the orbital period evolution (e.g. mass transfer, tides, etc.) are sub-dominant effects. Note that $\dot{f}_{\rm GW}$ is a difficult parameter for *LISA* to constrain, so chirp mass measurements are only possible for "outliers" of the total population, requiring high signal-to-noise (S/N), comparatively large $\dot{f}$, and/or long integration times for the *LISA* observations. Fortunately, due to the large number of detectable binaries, even the tails of the source distribution are well populated. The computation of the GW signal is only performed for the binaries with present-day frequency above 10^{-5} Hz.

3. Results

Fig. 2 shows the distributions of the He-He and CO-CO DWDs in the MW. The He-He DWDs distribution is almost spherical due to the bulge and halo, with a thick disk. On the opposite, the CO-CO DWDs are present almost exclusively in a very thin and elongated disk. The He-CO DWDs present an intermediate distribution, with prominent disk, although with a smaller scale height than for He-He DWDs, and a limited contribution from the bulge and halo.

Fig 3 shows the histogram of the frequency of the different types of binaries detected by *LISA*. This plot directly shows how the global frequency distribution in Fig. 3 translates into *LISA* detections. We find that He-CO DWDs and and He-He DWDs are the most numerous in the *LISA* band and among the detected sources, even though their contribution to the global galactic population is about 5% at most. This is because these binaries typically have the tightest orbits. He-He DWDs are present only up to about 5 mHz, because He WD have the largest radii. At higher frequencies, Roche Lobe overflow will happen and mass transfer will quickly become unstable and lead to a merger and we remove binaries above this frequency from our sample. The comparison between the resolved population (solid histogram in Fig. 3) and the complete DWD population in the galaxy (coloured lines) highlights that the sample of resolved binaries is complete down to 3 mHz, and even 2 mHz for the most massive binaries. Effectively, any binary with a period below 15 minutes will be individually resolvable, no matter its location in our galaxy, including the nearby satellites.

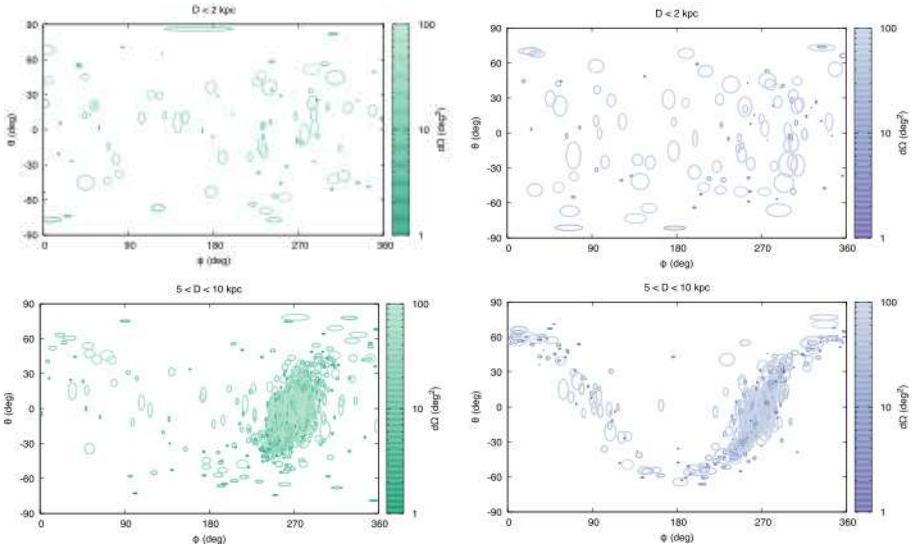

Fig. 4. Sky localisation in ecliptic coordinates for the well-localised binaries. The ellipses encompass the 1σ uncertainties on the inferred sky location, and the colour scale indicates the angular size of the error region in square degrees.

As such, all the detections of these systems will be crucial to constrain binary evolution.

The top row of Fig. 4 shows the sky localisation and its uncertainty for the different types of binaries within 2 kpc, which is roughly the distance where *Gaia* can observe WDs. About a 100 sources are likely present within this distance, with no preferred location. These objects could be found in the *Gaia* data using light-curves, particularly for the He-He binaries, which are likely to have the brightest EM counterparts. LSST will be able to detect DWDs up to roughly 10 kpc, which could yield a few thousand multi-messenger detections and reveal different sky localisations for different types of binaries.

4. Conclusions

LISA will individually resolve double white dwarfs with periods below 30 min. As the GW flux decreases as 1/r and GWs are not subject to crowding and dust obscuring, they are very complimentary to EM observations and will provide a new view of our Milky Way and its surrounding. LISA will effectively provide the first catalogue of white dwarf binaries complete up to periods of roughly 10 minutes. Many of these sources will be candidates for multi-messenger observations based on existing catalogues such as *Gaia* or high-cadence surveys such as LSST.

References

Amaro-Seoane, P., Audley, H., Babak, S., et al. 2017, arXiv: 1702.00786
Bellm, E. C., Kulkarni, S. R., Graham, M. J., et al. 2019, PASP, 131, 018002
Breivik, K., Kremer, K., Bueno, M., et al. 2018, ApJ, 854, L1
Brown, W. R., et al. 2016, ApJ, 818, 155
Brown, W. R., et al. 2010, ApJ, 723, 1072
Cooray, A. & Seto, N. 2005, ApJ, 623, L113
Cornish, N. J. & Littenberg, T. B. 2007, Phys. Rev. D, 76, 083006
Graham, M. J., Kulkarni, S. R., Bellm, E. C., et al. 2019, PASP, 131, 078001
Hopkins, P. F. 2015, MNRAS, 450, 53
Hopkins, P. F., Kereš, D., Oñorbe, J., et al. 2014, MNRAS, 445, 581
Hopkins, P. F., Wetzel, A., Kereš, D., et al. 2018, MNRAS, 480, 800
Hurley, J. R., Tout, C. A., & Pols, O. R. 2002, MNRAS, 329, 897

Ivanova, N., Justham, S., Chen, X., et al. 2013, A&A Rev., 21, 59
Korol, V., Koop, O., & Rossi, E. M. 2018, ApJ, 866, L20
Korol, V., Rossi, E. M., & Barausse, E. 2019, MNRAS, 483, 5518
Korol, V., Rossi, E. M., Groot, P. J., et al. 2017, MNRAS, 470, 1894
Kroupa, P. 2001, MNRAS, 322, 231
Kupfer, T., Korol, V., Shah, S., et al. 2018, MNRAS, 480, 302
Lamberts, A., Garrison-Kimmel, S., Hopkins, P. F., et al. 2018, MNRAS, 480, 2704
Levitan, D., Kupfer, T., Groot, P. J., et al. 2013, MNRAS, 430, 996
Ma, X., Hopkins, P. F., Wetzel, A. R., et al. 2017, MNRAS, 467, 2430
Napiwotzki, R., Christlieb, N., Drechsel, H., et al. 2001, Astronomische Nachrichten, 322, 411
Nelemans, G., et al. 2001a, A&A, 368, 939
Nelemans, G., Yungelson, L. R., & Portegies Zwart, S. F. 2001b, A&A, 375, 890
Nissanke, S., et al. 2012, ApJ, 758, 131
Postnov, K. A. & Yungelson, L. R. 2014, Living Reviews in Relativity, 17, 3
Ruiter, A. J., et al. 2009, ApJ, 693, 383
Ruiter, A. J., et al. 2010, ApJ, 717, 1006
Toonen, S., Hollands, M., Gänsicke, B. T., & Boekholt, T. 2017, A&A, 602, A16
Wetzel, A. R., Hopkins, P. F., Kim, J.-h., et al. 2016, ApJ, 827, L23
Yu, S. & Jeffery, C. S. 2013, MNRAS, 429, 1602